DOI:10.1002/cind.807_18.x

Biomedical

KEVIN BURGESS
Texas A&M University, US

Formation and *in situ* reactions of C-terminal peptides

Pentelute *et al*, in two consecutive papers, report systematic optimisation of acylation reactions of peptide electrophiles via acyl azides (*Org. Lett.*, doi: acs.orglett.5b03625 and 5b03626). Their message is that some hydrazides of peptides or proteins can be made chemoselectively, activated to acylazides via nitrous acid treatment, then reacted with good nucleophiles, particularly hydrazines, to give functionalised molecules. This concept is shown in Scheme 1a, while Scheme 1b shows how this approach was used to form peptides 'stapled' into helical conformations.

Chemoselective reductions of tertiary amides

Several years ago, the *Organometallic Highlights* column featured innovative work by Brookhart on catalysed hydrosilylation reactions to reduce amides. Tunnis, Adolfsson and co-workers have published related studies, which focus on secondary amides (*Angew. Chem. Int. Ed.*, 2016, **55**, 4562).

They report two reactions: one in which tertiary amides are cleaved to aldehydes and secondary amines, and another in which they are reduced to tertiary amines. An example of this is shown in Reaction 1, which nicely highlights synthesis of a pharmaceutical used in palliative care of Alzheimer's disease.

Targeting fluorescent probes *in vivo*

Using fluorescence microscopy to screen interactions of a library of fluorescent dyes with cells has proved amazingly productive, and several aspects of that work have been mentioned in previous contributions to *Highlights*.

One that was not covered before is by Yun, Chang and co-workers, involving discovery of a cyanine-derivative CDnir7 that accumulates in macrophages and can be used to image inflammation *in vivo* (*Chem. Commun.*, 2014, **50**, 6589).

In a more recent application of cyanine dyes *in vivo*, Braun et al produced the cyanine **1** wherein a cell penetrating peptide ensured entry of the dye into cells, and a good dienophile (*Theranostics*, 2016, **6**, 131). Inverse electron demand reactions were used to further functionalise this molecule with cytotoxic substances.

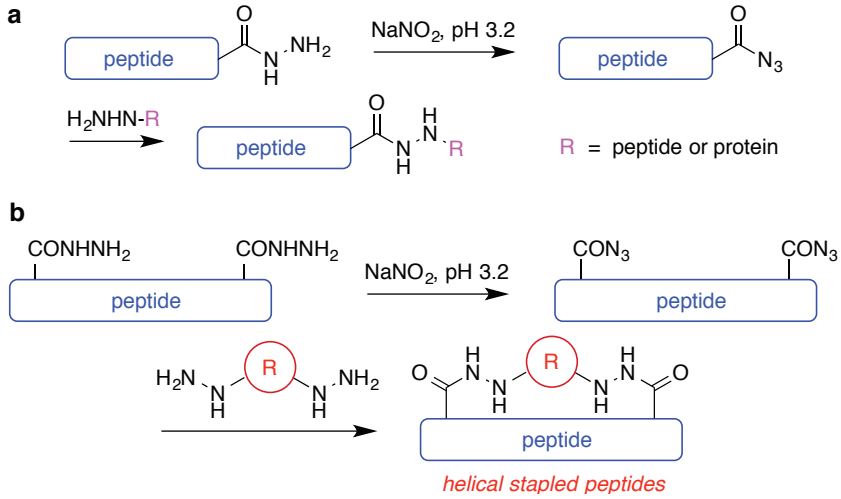

Scheme 1 ***a Activation and functionalisation of unprotected peptides and proteins; and, b use of this approach to make peptides with i – i + 4, or i – i + 7 side-chain linkages.***

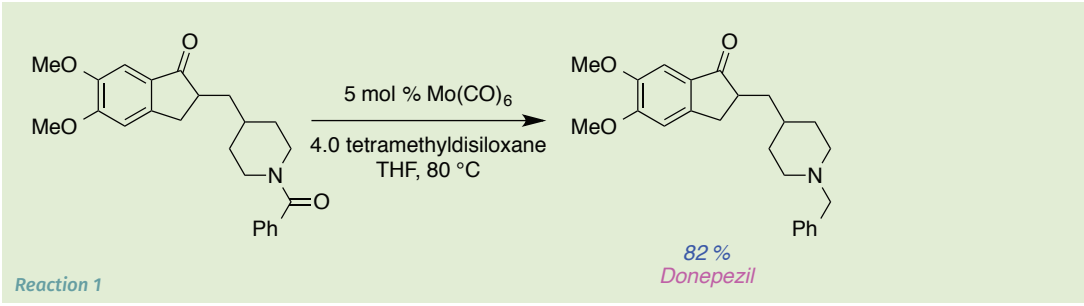

Reaction 1

Screening HDAC inhibitors in PEGA beads

Environments inside PEG-based polymeric beads are predominantly hydrophobic. Qvortrup and Nielsen recognised this and proved that a hydrophobic substance cleaved from a bead would remain in it if the surrounding environment is aqueous, but would be washed out quickly when the bead was placed in an organic medium (*Angew. Chem. Int. Ed.*, 2016, **55**, 4472).

Their proof of principle experiment involved testing histone deacylase (HDAC) enzymes. They captured a known inhibitor and a substrate in one bead type, and a non-inhibitor and substrate in another. Throughout, the unchanged substrate liberates a fluor when treated with trypsin. Treatment with both types of beads with an HDAC gave fluorescence only in the bead without the inhibitor.

The authors claim to be able to

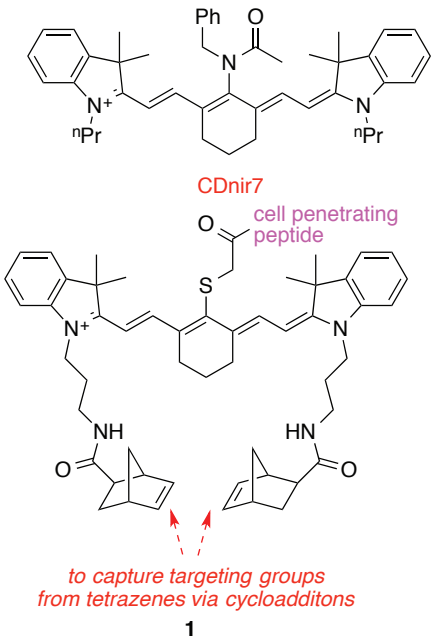

1

obtain dose-response curves where the photolysis time correlates to the amount of inhibitor liberated into the bead. These results are remarkable and surprising because enzymes are hydrophilic and do not tend to permeate into PEG-based beads.

Substrates on the surface of beads should be far more accessible to enzymes in solution than substrates at the core of the beads, so getting reproducible results might have been difficult; it will be interesting to see if this approach can be applied to other systems.

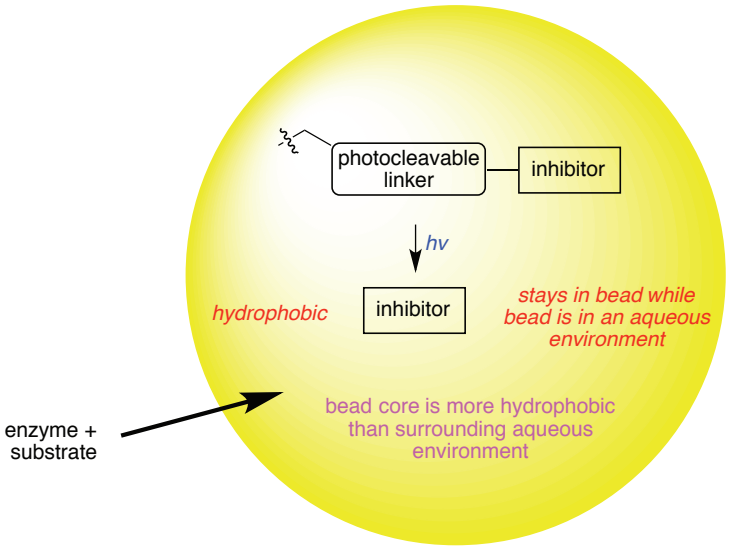

Applied chemistry

NIGEL P FREESTONE
University of Northampton, UK

Tyre recycling

UK scientists have developed a chemical route that breaks down the base rubber in tyres into useful materials, at room temperature (R. F. Smith, S. C. Boothroyd, R. L. Thompson, E. Khosravi; *Green Chem.*, doi: 10.1039/C5GC03075G) (Scheme 1).

Tyres are difficult to dispose of because of their awkward shape and leachable toxins. They can be recycled by cutting or grinding into 'rubber crumb' for use as a building material, or by heating in an oxygen free environment to make crude fuels; both are energy intensive.

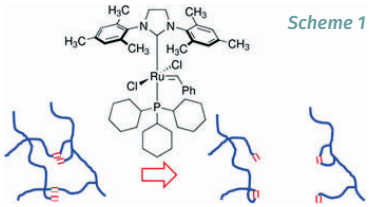

Scheme 1

The new approach breaks down styrene butadiene rubber at room temperature and without mechanical input, by placing it in dichloromethane with a ruthenium-based Grubbs' catalyst. As crosslinks in the rubber network are cleaved and polymer chains fragment into smaller chains, the material physically disintegrates into rubber crumb. By allowing the reaction to continue, the material can be further broken down into an oil comprised of low molecular weight oligomers. In theory, these could be repolymerised into a new rubber product with different properties.

Adhesive elastomeric supramolecular polyurethane healable at body temperature

Scheme 2

An adhesive and elastic polymer that repairs itself at body temperature, has been reported, which could modernise wound dressings and regenerative medicines such as artificial skin (A. Feula, X. Tang, I. Giannakopoulos, A. M. Chippindale, I. W. Hamley, F. Greco, C. P. Buckley, C. R. Siviourb, W. Hayes; *Chem. Sci.*, doi: 10.1039/C5SC04864H) (Scheme 2).

When cut with a razor, strips of the non-cytotoxic polyurethane network material flow back together as its supramolecular network has been disrupted, lowering viscosity at the affected area. The material is stable under simulated physiological conditions and initial testing on human skin cells suggests it would be safe for medical use. The polymer also retains its self-healing ability when adhered to pig skin.

Silicon nanosheets

Silicon nanosheets have attracted much attention owing to their novel electronic and optical properties and compatibility with existing silicon technology. However, a cost-effective and scalable technique for synthesising these nanosheets remains elusive.

A novel strategy for producing silicon nanosheets on a large scale through the simultaneous molten-salt-induced exfoliation and chemical reduction of natural clay has been developed (J. Ryu, Y. J. Jang, S. Choi, H. J. Kang, H. Park, J. S. Lee, S. Park; *NPG Asia Materials*, doi:10.1038/am.2016.35).

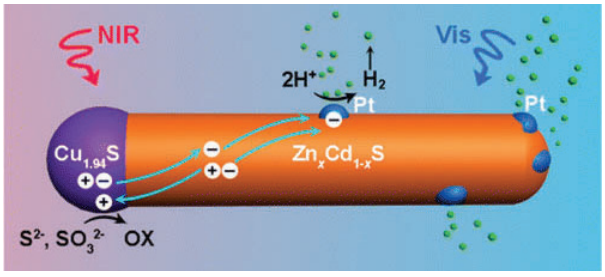

Scheme 3

The silicon nanosheets thus produced have a high surface area, are ultrathin (~5nm) and contain mesoporous structures derived from the oxygen vacancies in the clay. These advantages make the nanosheets a highly suitable photocatalyst with an exceptionally high activity for the generation of hydrogen from a water–methanol mixture.

Further, when the silicon nanosheets are combined with platinum as a cocatalyst, they exhibit high activity in KOH (15.83 mmol H_2/s/

mol Si) and excellent photocatalytic activity with respect to the evolution of hydrogen from a water–methanol mixture (723 µmol H_2/h/g Si).

Heteronanorod hydrogen generators

The heteronanorods $Cu_{1.94}S–Zn_xCd_{1-x}S$ (0≤ x ≤1) possess two light absorbers; intimate heterointerfaces; tunable band gaps over a wide range; and uniform one-dimensional morphology (Y. Chen, S. Zhao, X. Wang ||, Q. Peng, R. Lin, Y. Wang, R. Shen, X. Cao, L. Zhang, G. Zhou, J. Li, A. Xia||, Y. Li; *J. Am. Chem. Soc.*, 2016, **138**, 4286) (Scheme 3).

Even without any cocatalysts, $Cu_{1.94}S–Zn_{0.23}Cd_{0.77}S$ heteronanorods exhibit efficient hydrogen production activity (7735µmolh^{-1}g^{-1}) under visible-light irradiation (λ>420nm), representing a 59-fold enhancement, compared with the pristine CdS catalyst.

Meanwhile, deposition of a Pt cocatalyst on the $Cu_{1.94}SZn_xCd_{1-x}S$ surface substantially enhances the hydrogen production performance (13 533µmolh^{-1}g^{-1}) with an apparent quantum efficiency of 26.4% at 420nm, opening up opportunities to promote the overall photocatalytic performance using rationally designed nanostructures.

Smart bandages

Capsules for use in bandages that can store antibacterials and control their activity, aiding in the fight against antimicrobial resistance are now available (M. Liu, F. Fang, X. Song, F. Yu, F. Li, X. Shi, C. Xue, T. Chenb, X. Wang; *J. Mater. Chem. B*, 2016, 4, 2544) (Scheme 4).

Bacterial strains resilient towards multiple drugs are an increasingly common and dangerous part of the 21st century. With repercussions global in scale, innovative devices are needed that deliver antibacterial agents precisely and instantly so bacteria cannot adapt.

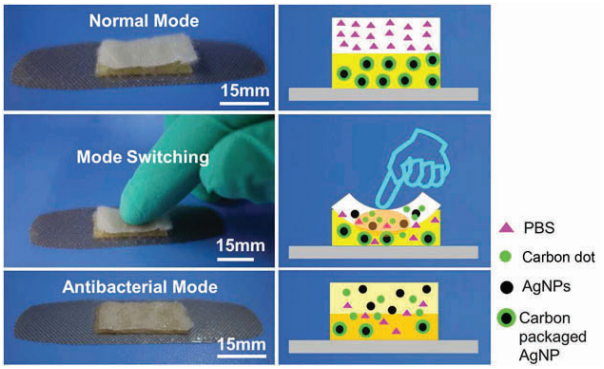

Scheme 4 ***The smart bandage contains silver nanoparticles (AgNPs) packaged in carbon below a layer of phosphate buffered saline (PBS). Pressing the bandage causes the layers to interact, releasing the antibacterial silver particles***

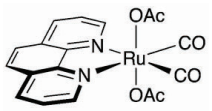

Scheme 5

The new switchable supramolecular capsules are based on silver nanoparticles enclosed in carbon membranes. They regulate the activity of the antibacterial silver so that it possesses three distinct and switchable modes – packaged, on and off – with the added bonus that the materials can be 3D printed into a variety of shapes, such as smart caps for culture bottles.

To demonstrate the capsules' features, the research team incorporated them into plasters. The resulting intelligent bandages have two pieces, a top layer containing sterilised phosphate buffered saline and a bottom layer containing the antibacterial capsules. A simple press of the bandage causes the layers to interact, releasing the active silver particles and changing the colour from white to orange, showing the bandage is on. The particles' antibacterial action switches off if they aggregate together.

New catalyst releases more hydrogen from ammonia borane

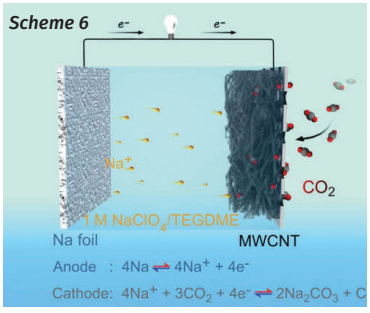

Scientists are a step closer to ammonia borane-powered fuel cells thanks to a ruthenium catalyst that yields an unprecedented amount of hydrogen. Ammonia borane (AB) has high hydrogen density (19.6wt%), and can, in principle, release up to 3 equivalents of H_2 under mild catalytic conditions. However, borazine results from ammonia borane releasing two hydrogen molecules, limiting the capacity of fuel cells capacity. Borazine can also poison fuel cells by deactivating the catalyst, and is resistant to further hydrogen release.

There are a limited number of catalysts are capable of non-hydrolytic dehydrogenation of AB beyond 2 equivalents of H_2 under mild conditions, but none of these is shown directly to derivatise borazine. A new high productivity ruthenium-based catalyst, $\{(phen)Ru(OAc)_2(CO)_2\}$ that effects AB dehydrogenation through 2.7 equivalents of H_2 at 70°C, which is both robust and is water and air stable, has been reported (X Zhang, L. Kam and T. J. Williams, *Dalton Trans.*, 2016, **45**, 7672) (Scheme 5).

Since the catalyst both dehydrogenates borazine in isolation and dehydrogenates AB itself, borazine formation no longer limits ammonia borane's hydrogen releasing potential.

Rechargeable sodium-carbon battery

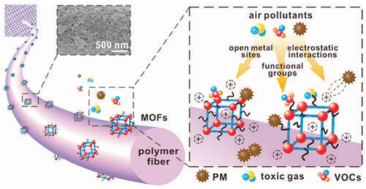

Scheme 7

The first rechargeable sodium–carbon dioxide battery has been created with the help of a nanostructured cathode (X. Hu, J. Sun, Z. Li, Q. Zhao, C. Chen, J. Chen; *Angew. Chem. Int. Ed. Engl. Eng.*, 2016, **55**, 6482) (Scheme 6).

This cheap and potentially powerful battery could fuel Mars vehicles as the red planet's atmosphere is 96% carbon dioxide or recycle carbon dioxide emissions on Earth.

The battery comprises a Na-foil anode; glass fibre separator; ether-based electrolyte; and a tetraethylene glycol dimethyl-treated multi-wall carbon nanotube (t-MWCNT) cathode on Ni mesh without binder addition. During discharge, CO_2 reacts with Na to form polycrystalline Na_2CO_3 and amorphous C. During charging, the reversible reaction is taking place.

The as-prepared Na–CO_2 batteries display high electrochemical performance, including large reversible capacity (60 000mAh g^{-1}); high rate capability (4A g^{-1} with capacity of 4000mAh g^{-1}); a small discharge/charge voltage gap (0.6V); and superior cyclability of 200 cycles at 1Ag^{-1}.

Metal–organic framework filters for efficient air pollution control

Environmental challenges especially air pollution (particulate matter (PM) and toxic gases) pose serious

threats to public health globally. Metal–organic frameworks (MOFs) are crystalline materials with high porosity, tunable pore size, and rich functionalities, holding the promise of capture for poisonous pollutants (Y. Zhang, S. Yuan, X. Feng, H. Li, J. Zhou, B. Wang; *J. Amer. Chem. Soc.*, 2016, **138**, 5785) (Scheme 7).

Processing nanocrystals of four unique MOF structures into nanofibrous filters (MOF loadings up to 60wt%) produces a material that exhibits high PM removal efficiencies up to 88.33±1.52% and 89.67±1.33% for PM2.5 and PM10, respectively. These thin MOFilters can further selectively capture and retain SO_2 when exposed to a stream of SO_2/N_2 mixture, and their hierarchical nanostructures can easily permeate fresh air at high gas flow rate with the pressure drop <20Pa.

MIP deodorants

French researchers at the Compiègne University of Technology and L'Oréal have incorporated molecularly imprinted polymers (MIPs) – dubbed 'plastic antibodies' – into a cosmetic product to capture precursor chemicals in human sweat that cause bad smells (S. Nestora, F. Merlier, S. Beyazit, E. Prost, L. Duma, B. Baril, A. Greaves, K. Haupt, B. T. S. Bui; *Angew Chem Int Ed Engl.*, 2016, **55**, 6252) (Scheme 8).

Skin bacteria transform some of the secreted, odourless chemicals of sweat into molecules that smell. Deodorants usually work by killing these bacteria with bactericides, including triclosan and chlorhexidine. Anti-perspirants block the flow of sweat with aluminium salts, which also have antibacterial properties. MIPs provide an alternative deodorant principle. The idea is to prevent the formation of body odors without disturbing the fragile microbial equilibrium of the skin.

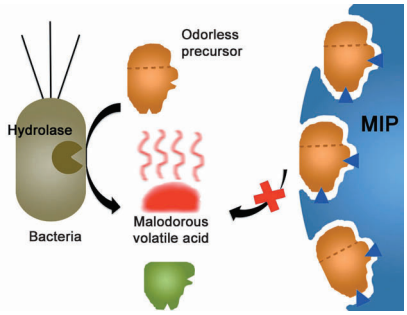

Scheme 8

This is achieved by using a MIP as a specific scavenger agent to trap non-odorous precursors of malodours, thus preventing them from being transformed by skin bacteria into volatile malodorous compounds. The MIPs in the new formulation selectively scavenges and inactivates the precursors of bad smells, without disturbing the skin microbiota.

To create the MIP, the researchers searched for a functional analogue of the glutamine precursors of two smelly molecules and settled on Nα-hexanoyl glutamic acid. They then polymerised the monomer 4-acrylamidophenyl(amino) methaniminium acetate with this compound to make a powdered MIP with binding cavities complementary in shape, size and functional group orientation to the molecule.

While inclusion of such MIPs in a cosmetic product will require much formulation development, it is clear to see the potential of imprinting technology in a range of topical applications, both cosmetic and therapeutic.

Scheme 9

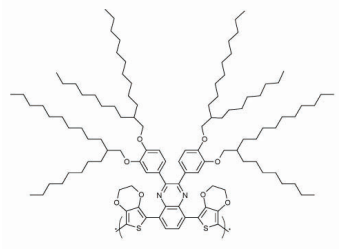

Colour-changing polymer adapts camouflage to vegetation and desert

Chinese scientists are closer to producing outfits for the armed forces that change colour to match surroundings when soldiers move from a forest to a desert, having designed an organic polymer that is green in the reduced state but when a low voltage is applied, oxidises to a sandy-brown colour (H. Yu *et al*, *J. Mater. Chem. C*, 2016, **4**, 2269) (Scheme 9).

Switching between colours takes 1–1.5 seconds and is maintained after 1000 repetitions. The polymer can be readily incorporated into clothing by simply spraying conductive fabric with a mixture of the polymer and toluene. Since the polymer also absorbs IR radiation, it could conceal body heat too, and given its super-hydrophobic behaviour, it would not wash out of clothing.

Organic chemistry

G. RICHARD STEPHENSON
University of East Anglia, UK

Chiral diversity

Chirality is the property of 'handedness' applied at the molecular scale, but when chemistry is involved (Figure 1), there is more to 'handedness' than just having left or right hands. Best known, of course, are atom-centred forms of chirality, such as, in organic chemistry, the classic tertasubstituted stereogenic center (a 'chiral centre') at carbon. However, it is also possible to envisage axial chirality and helical chirality (sometimes referred to as 'planar chirality' because two sides of an unsymmetrical plane within the molecule are differentiated by structural features).

These concepts have been brought together in a single cage molecule which, as a consequence, has a very unusual unsymmetrical environment inside its cavity (D. Zhang, J.-C. Mulatier, J. R. Cochrane, L. Guy, G. Gao, J.-P. Dutasta, A. Martinez, *Chem. Eur. J.* 2016, **22**, 8038–8042).

In the lower section (Scheme 1), there is a ring of three OH groups, which are beautifully placed to promote cooperative C_3 symmetric multiple hydrogen bonding interactions. These are based on a set of three stereogenic carbons, introduced in the synthesis by choosing (S)-(+)-glycidyl nosylate as a starting material.

In contrast, the upper section of the cavity is closed by a cyclotriveratrylene (CTV) circle of three aromatic rings joined by CH_2 groups. Here, the alternating pattern of OMe and OR groups on the CTV establishes the helicity of the chirality, since the puckered CH_2 links between adjacent arenes ensure that they do not lie in the same plane. Thus the top (3 CH_2s) and bottom (3

HC=C(OMe)-C(OR)=CHs) of these CVTs are different.

Sequencing pharmacophores in rings

Bioactive multifunctional macrocycles are catching the attention of synthetic chemists and pose a new challenge if a selection of different, potentially bioactive, pharmaocphores are to be included; it is a question of getting the order right (Figure 2).

Such structures can emulate the selective multiple interactions of the amino acid side-chain functionality of natural antimicrobial peptides, but with a far greater potential for structural diversity, and the possibility of better *in vivo* stability and pharmacodymanics (M. Porel, D. N. Thornlow, N. N. Phan, C. A. Alabi, *Nature Chem.* 2016, **8**, 590-596).

In this work, the key to the synthesis of the sequence-defined structures has been to apply a one-pot acid-catalysed cascade reaction.

With this work, the urgent quest for new antimicrobial compounds and has not just taken a new turn, it has made a new ring.

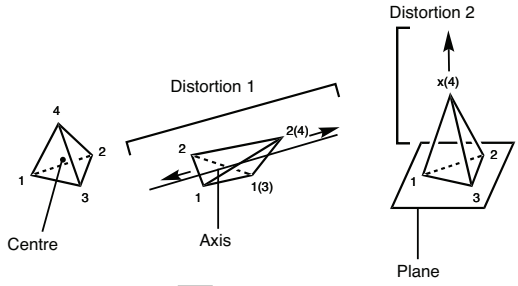

Figure 1 ***A regular tetrahedron and distortions that separate opposite edges (distortion 1) or one corner from a plane (distortion 2). The centre of the regular tetrahedron, the axis identified by distortion 1, and the plane identified by distortion 2, illustrate the chiral properties of these three-dimensional forms (for chirality to be present, all four corners need to be different in the regular tetrahedron, only two pairs of corners need to be different in the axial case, and just the three corners in the plane need to be different in the planar case)***

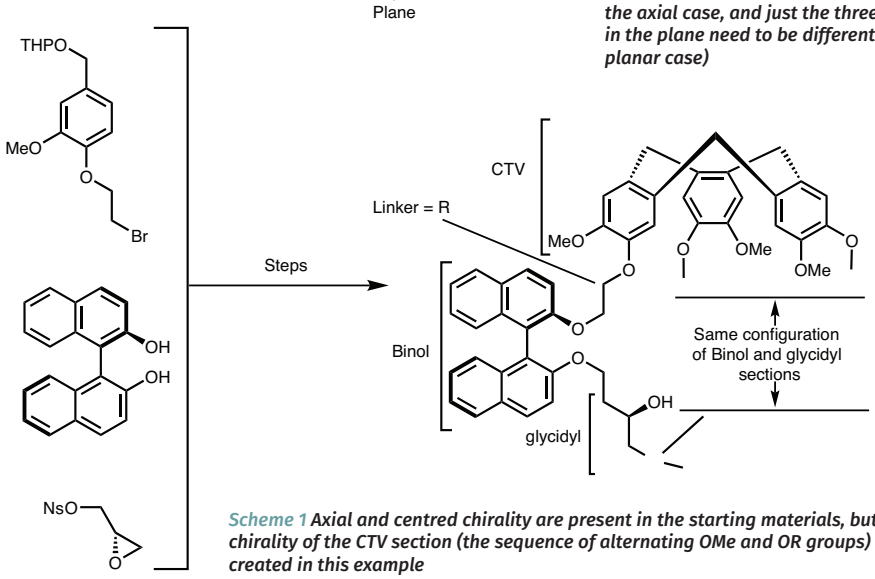

Scheme 1 ***Axial and centred chirality are present in the starting materials, but planar chirality of the CTV section (the sequence of alternating OMe and OR groups) is also created in this example***

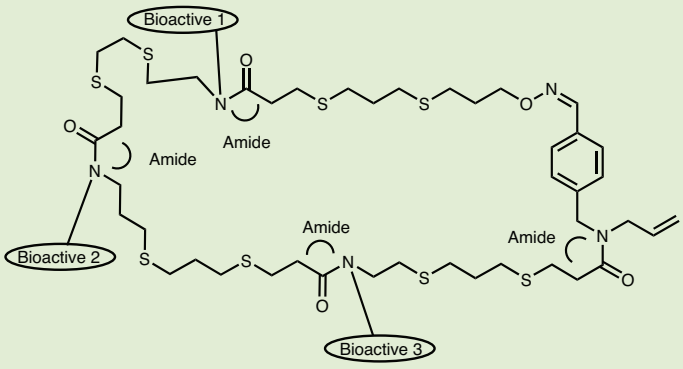

Figure 2 ***Three bioactive groups in sequence within a cyclic tetrapeptide joined by four amide links***

Cross-coupling of anisoles

Ethers are usually thought of as inert functional groups, and in the context of metal-catalysed coupling chemistry, the gradual diversification of types of functionality that are practical for oxidative addition (the typical first step in the catalytic cycle) had, in the O-linked series, stopped at triflates and similar quite reactive functionality.

Now, a nickel-catalysed system has been found that accepts anisole as its aromatic starting material (M. Tobisu, T. Takahira, T. Morioka, N. Chatani, *J. Am. Chem. Soc.*, 2016, **138**, 6711–6714).

The reaction conditions employ $Ni(cod)_2$ in combination with 1,2-bis(dicyclohexylphosphino)ethane (dcype) and Grigrard reagents, and the generality of the procedure has been exemplified with a wide range of MeO-substituted aromatic rings. The example in Scheme 2 shows its use in a reaction sequence where the normal chemical stability of the anisole derivative is important prior to the nickel-catalysed step.

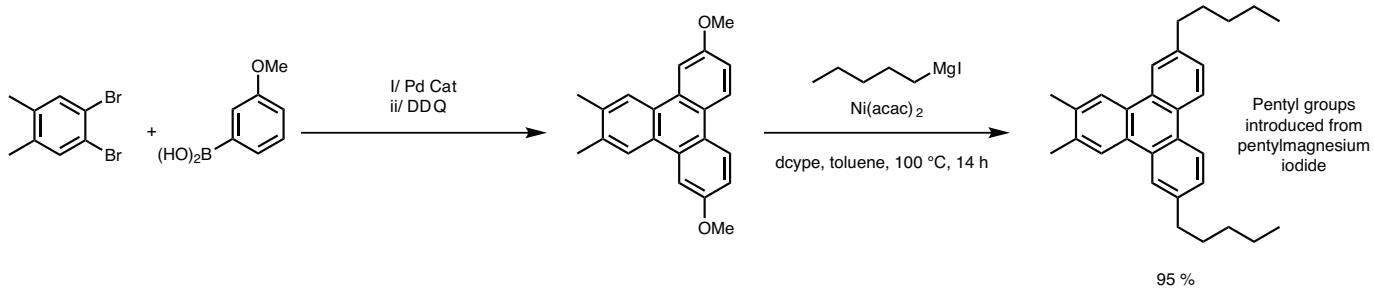

Scheme 2 ***An example of a nickel catalysed reaction that replaces an aryl OMe group by the pentyl group from pentylmagnesium iodide. After the initial conventional palladium-catalysed double Suzuki coupling, the stability of the OMe groups is crucial to the success of the harsh oxidising conditions (DDQ) used for the cyclisation step. From this well established entry route, a wide variety of different substitution patterns are now accessible by the correct choice of Grignard reagent.***